

# First measurement of neutrino oscillation parameters using neutrinos and antineutrinos by NOvA

M. A. Acero,<sup>2</sup> P. Adamson,<sup>12</sup> L. Aliaga,<sup>12</sup> T. Alion,<sup>39</sup> V. Allakhverdian,<sup>27</sup> S. Altakarli,<sup>46</sup> N. Anfimov,<sup>27</sup> A. Antoshkin,<sup>27,31</sup> A. Aurisano,<sup>6</sup> A. Back,<sup>24</sup> C. Backhouse,<sup>44</sup> M. Baird,<sup>19,39,45</sup> N. Balashov,<sup>27</sup> P. Baldi,<sup>25</sup> B. A. Bambah,<sup>17</sup> S. Bashar,<sup>43</sup> K. Bays,<sup>4,21</sup> S. Bending,<sup>44</sup> R. Bernstein,<sup>12</sup> V. Bhatnagar,<sup>32</sup> B. Bhuyan,<sup>14</sup> J. Bian,<sup>25,31</sup> T. Blackburn,<sup>39</sup> J. Blair,<sup>16</sup> A. C. Booth,<sup>39</sup> P. Bour,<sup>9</sup> C. Bromberg,<sup>29</sup> N. Buchanan,<sup>8</sup> A. Butkevich,<sup>22</sup> S. Calvez,<sup>8</sup> M. Campbell,<sup>44</sup> T. J. Carroll,<sup>42</sup> E. Catano-Mur,<sup>24,47</sup> A. Cedeno,<sup>46</sup> S. Childress,<sup>12</sup> B. C. Choudhary,<sup>11</sup> B. Chowdhury,<sup>35</sup> T. E. Coan,<sup>37</sup> M. Colo,<sup>47</sup> J. Cooper,<sup>12</sup> L. Corwin,<sup>36</sup> L. Cremonesi,<sup>44</sup> G. S. Davies,<sup>19</sup> P. F. Derwent,<sup>12</sup> P. Ding,<sup>12</sup> Z. Djurcic,<sup>1</sup> D. Doyle,<sup>8</sup> E. C. Dukes,<sup>45</sup> H. Duyang,<sup>35</sup> S. Edayath,<sup>7</sup> R. Ehrlich,<sup>45</sup> M. Elkins,<sup>24</sup> G. J. Feldman,<sup>15</sup> P. Filip,<sup>23</sup> W. Flanagan,<sup>10</sup> M. J. Frank,<sup>34,45</sup> H. R. Gallagher,<sup>43</sup> R. Gandrajula,<sup>29</sup> F. Gao,<sup>33</sup> S. Germani,<sup>44</sup> A. Giri,<sup>18</sup> R. A. Gomes,<sup>13</sup> M. C. Goodman,<sup>1</sup> V. Grichine,<sup>28</sup> M. Groh,<sup>19</sup> R. Group,<sup>45</sup> B. Guo,<sup>35</sup> A. Habig,<sup>30</sup> F. Haki,<sup>20</sup> J. Hartnell,<sup>39</sup> R. Hatcher,<sup>12</sup> A. Hatzikoutelis,<sup>41</sup> K. Heller,<sup>31</sup> V. Hewes,<sup>6</sup> A. Himmel,<sup>12</sup> A. Holin,<sup>44</sup> B. Howard,<sup>19</sup> J. Huang,<sup>42</sup> J. Hylen,<sup>12</sup> F. Jediny,<sup>9</sup> C. Johnson,<sup>8</sup> M. Judah,<sup>8</sup> I. Kakorin,<sup>27</sup> D. Kalra,<sup>32</sup> D. M. Kaplan,<sup>21</sup> R. Keloth,<sup>7</sup> O. Klimov,<sup>27</sup> L. W. Koerner,<sup>16</sup> L. Kolupaeva,<sup>27</sup> S. Kotelnikov,<sup>28</sup> A. Kreymer,<sup>12</sup> Ch. Kulenberg,<sup>27</sup> A. Kumar,<sup>32</sup> C. D. Kuruppu,<sup>35</sup> V. Kus,<sup>9</sup> T. Lackey,<sup>19</sup> K. Lang,<sup>42</sup> S. Lin,<sup>8</sup> M. Lokajicek,<sup>23</sup> J. Lozier,<sup>4</sup> S. Luchuk,<sup>22</sup> K. Maan,<sup>32</sup> S. Magill,<sup>1</sup> W. A. Mann,<sup>43</sup> M. L. Marshak,<sup>31</sup> M. Martinez-Casales,<sup>24</sup> V. Matveev,<sup>22</sup> D. P. Méndez,<sup>39</sup> M. D. Messier,<sup>19</sup> H. Meyer,<sup>46</sup> T. Miao,<sup>12</sup> W. H. Miller,<sup>31</sup> S. R. Mishra,<sup>35</sup> A. Mislivec,<sup>31</sup> R. Mohanta,<sup>17</sup> A. Moren,<sup>30</sup> L. Muallem,<sup>4</sup> M. Muether,<sup>46</sup> S. Mufson,<sup>19</sup> K. Mulder,<sup>44</sup> R. Murphy,<sup>19</sup> J. Musser,<sup>19</sup> D. Naples,<sup>33</sup> N. Nayak,<sup>25</sup> J. K. Nelson,<sup>47</sup> R. Nichol,<sup>44</sup> G. Nikseresht,<sup>21</sup> E. Niner,<sup>12</sup> A. Norman,<sup>12</sup> T. Nosek,<sup>5</sup> A. Olshevskiy,<sup>27</sup> T. Olson,<sup>43</sup> J. Paley,<sup>12</sup> R. B. Patterson,<sup>4</sup> G. Pawloski,<sup>31</sup> D. Pershey,<sup>4</sup> O. Petrova,<sup>27</sup> R. Petti,<sup>35</sup> D. D. Phan,<sup>42</sup> R. K. Plunkett,<sup>12</sup> B. Potukuchi,<sup>26</sup> C. Principato,<sup>45</sup> F. Psihas,<sup>19</sup> A. Radovic,<sup>47</sup> V. Raj,<sup>4</sup> R. A. Rameika,<sup>12</sup> B. Rebel,<sup>12,48</sup> P. Rojas,<sup>8</sup> V. Ryabov,<sup>28</sup> O. Samoylov,<sup>27</sup> M. C. Sanchez,<sup>24</sup> S. Sánchez Falero,<sup>24</sup> I. S. Seong,<sup>25</sup> P. Shanahan,<sup>12</sup> A. Sheshukov,<sup>27</sup> P. Singh,<sup>11</sup> V. Singh,<sup>3</sup> E. Smith,<sup>19</sup> J. Smolik,<sup>9</sup> P. Snopok,<sup>21</sup> N. Solomey,<sup>46</sup> E. Song,<sup>45</sup> A. Sousa,<sup>6</sup> K. Soustruznik,<sup>5</sup> M. Strait,<sup>31</sup> L. Suter,<sup>12</sup> A. Sutton,<sup>45</sup> R. L. Talaga,<sup>1</sup> B. Tapia Oregui,<sup>42</sup> P. Tas,<sup>5</sup> R. B. Thayyullathil,<sup>7</sup> J. Thomas,<sup>44,48</sup> E. Tiras,<sup>24</sup> D. Torbunov,<sup>31</sup> J. Tripathi,<sup>32</sup> A. Tsaris,<sup>12</sup> Y. Torun,<sup>21</sup> J. Urheim,<sup>19</sup> P. Vahle,<sup>47</sup> J. Vasek,<sup>19</sup> L. Vinton,<sup>39</sup> P. Vokac,<sup>9</sup> T. Vrba,<sup>9</sup> M. Wallbank,<sup>6</sup> B. Wang,<sup>37</sup> T. K. Warburton,<sup>24</sup> M. Wetstein,<sup>24</sup> M. While,<sup>36</sup> D. Whittington,<sup>40,19</sup> S. G. Wojcicki,<sup>38</sup> J. Wolcott,<sup>43</sup> N. Yadav,<sup>14</sup> A. Yallappa Dombara,<sup>40</sup> K. Yonehara,<sup>12</sup> S. Yu,<sup>1,21</sup> S. Zadorozhnyy,<sup>22</sup> J. Zalesak,<sup>23</sup> B. Zamorano,<sup>39</sup> and R. Zwaska<sup>12</sup>

(The NOvA Collaboration)

<sup>1</sup>Argonne National Laboratory, Argonne, Illinois 60439, USA

<sup>2</sup>Universidad del Atlantico, Km. 7 antigua via a Puerto Colombia, Barranquilla, Colombia

<sup>3</sup>Department of Physics, Institute of Science, Banaras Hindu University, Varanasi, 221 005, India

<sup>4</sup>California Institute of Technology, Pasadena, California 91125, USA

<sup>5</sup>Charles University, Faculty of Mathematics and Physics, Institute of Particle and Nuclear Physics, Prague, Czech Republic

<sup>6</sup>Department of Physics, University of Cincinnati, Cincinnati, Ohio 45221, USA

<sup>7</sup>Department of Physics, Cochin University of Science and Technology, Kochi 682 022, India

<sup>8</sup>Department of Physics, Colorado State University, Fort Collins, CO 80523-1875, USA

<sup>9</sup>Czech Technical University in Prague, Brehova 7, 115 19 Prague 1, Czech Republic

<sup>10</sup>University of Dallas, 1845 E Northgate Drive, Irving, Texas 75062 USA

<sup>11</sup>Department of Physics and Astrophysics, University of Delhi, Delhi 110007, India

<sup>12</sup>Fermi National Accelerator Laboratory, Batavia, Illinois 60510, USA

<sup>13</sup>Instituto de Física, Universidade Federal de Goiás, Goiânia, Goiás, 74690-900, Brazil

<sup>14</sup>Department of Physics, IIT Guwahati, Guwahati, 781 039, India

<sup>15</sup>Department of Physics, Harvard University, Cambridge, Massachusetts 02138, USA

<sup>16</sup>Department of Physics, University of Houston, Houston, Texas 77204, USA

<sup>17</sup>School of Physics, University of Hyderabad, Hyderabad, 500 046, India

<sup>18</sup>Department of Physics, IIT Hyderabad, Hyderabad, 502 205, India

<sup>19</sup>Indiana University, Bloomington, Indiana 47405, USA

<sup>20</sup>Institute of Computer Science, The Czech Academy of Sciences, 182 07 Prague, Czech Republic

<sup>21</sup>Department of Physics, Illinois Institute of Technology, Chicago IL 60616, USA

<sup>22</sup>Inst. for Nuclear Research of Russia, Academy of Sciences 7a, 60th October Anniversary prospect, Moscow 117312, Russia

<sup>23</sup>Institute of Physics, The Czech Academy of Sciences, 182 21 Prague, Czech Republic

<sup>24</sup>Department of Physics and Astronomy, Iowa State University, Ames, Iowa 50011, USA

<sup>25</sup>Department of Physics and Astronomy, University of California at Irvine, Irvine, California 92697, USA

- <sup>26</sup>Department of Physics and Electronics, University of Jammu, Jammu Tawi, 180 006, Jammu and Kashmir, India  
<sup>27</sup>Joint Institute for Nuclear Research, Dubna, Moscow region 141980, Russia  
<sup>28</sup>Nuclear Physics and Astrophysics Division, Lebedev Physical Institute, Leninsky Prospect 53, 119991 Moscow, Russia  
<sup>29</sup>Department of Physics and Astronomy, Michigan State University, East Lansing, Michigan 48824, USA  
<sup>30</sup>Department of Physics and Astronomy, University of Minnesota Duluth, Duluth, Minnesota 55812, USA  
<sup>31</sup>School of Physics and Astronomy, University of Minnesota Twin Cities, Minneapolis, Minnesota 55455, USA  
<sup>32</sup>Department of Physics, Panjab University, Chandigarh, 160 014, India  
<sup>33</sup>Department of Physics, University of Pittsburgh, Pittsburgh, Pennsylvania 15260, USA  
<sup>34</sup>Department of Physics, University of South Alabama, Mobile, Alabama 36688, USA  
<sup>35</sup>Department of Physics and Astronomy, University of South Carolina, Columbia, South Carolina 29208, USA  
<sup>36</sup>South Dakota School of Mines and Technology, Rapid City, South Dakota 57701, USA  
<sup>37</sup>Department of Physics, Southern Methodist University, Dallas, Texas 75275, USA  
<sup>38</sup>Department of Physics, Stanford University, Stanford, California 94305, USA  
<sup>39</sup>Department of Physics and Astronomy, University of Sussex, Falmer, Brighton BN1 9QH, United Kingdom  
<sup>40</sup>Department of Physics, Syracuse University, Syracuse NY 13210, USA  
<sup>41</sup>Department of Physics and Astronomy, University of Tennessee, Knoxville, Tennessee 37996, USA  
<sup>42</sup>Department of Physics, University of Texas at Austin, Austin, Texas 78712, USA  
<sup>43</sup>Department of Physics and Astronomy, Tufts University, Medford, Massachusetts 02155, USA  
<sup>44</sup>Physics and Astronomy Dept., University College London, Gower Street, London WC1E 6BT, United Kingdom  
<sup>45</sup>Department of Physics, University of Virginia, Charlottesville, Virginia 22904, USA  
<sup>46</sup>Department of Mathematics, Statistics, and Physics, Wichita State University, Wichita, Kansas 67206, USA  
<sup>47</sup>Department of Physics, College of William & Mary, Williamsburg, Virginia 23187, USA  
<sup>48</sup>Department of Physics, University of Wisconsin-Madison, Madison, Wisconsin 53706, USA

The NOvA experiment has made a  $4.4\sigma$ -significant observation of  $\bar{\nu}_e$  appearance in a 2 GeV  $\bar{\nu}_\mu$  beam at a distance of 810 km. Using  $12.33 \times 10^{20}$  protons on target delivered to the Fermilab NuMI neutrino beamline, the experiment recorded 27  $\bar{\nu}_\mu \rightarrow \bar{\nu}_e$  candidates with a background of 10.3 and 102  $\bar{\nu}_\mu \rightarrow \bar{\nu}_\mu$  candidates. This new antineutrino data is combined with neutrino data to measure the oscillation parameters  $|\Delta m_{32}^2| = 2.48_{-0.06}^{+0.11} \times 10^{-3} \text{ eV}^2/c^4$ ,  $\sin^2 \theta_{23} = 0.56_{-0.03}^{+0.04}$  in the normal neutrino mass hierarchy and upper octant and excludes most values near  $\delta_{\text{CP}} = \pi/2$  for the inverted mass hierarchy by more than  $3\sigma$ . The data favor the normal neutrino mass hierarchy by  $1.9\sigma$  and  $\theta_{23}$  values in the upper octant by  $1.6\sigma$ .

The observations of neutrino oscillations by many experiments [1–9] are well described by the mixing of three neutrino mass eigenstates  $\nu_1$ ,  $\nu_2$ , and  $\nu_3$  with the flavor eigenstates  $\nu_e$ ,  $\nu_\mu$ , and  $\nu_\tau$ . The mixing is parameterized by a unitary matrix,  $U_{\text{PMNS}}$ , which depends on three angles and a phase,  $\delta_{\text{CP}}$ , that may break Charge-Parity (CP) symmetry. The oscillation frequencies are proportional to the neutrino mass splittings,  $\Delta m_{21}^2 \equiv m_2^2 - m_1^2 \simeq 7.5 \times 10^{-5} \text{ eV}^2/c^4$  and  $|\Delta m_{32}^2| \simeq 2.5 \times 10^{-3} \text{ eV}^2/c^4$ , and the angles are known to be large:  $\theta_{12} \simeq 34^\circ$ ,  $\theta_{13} \simeq 8^\circ$ ,  $\theta_{23} \simeq 45^\circ$  [10];  $\delta_{\text{CP}}$ , however, is largely unknown.

Within this framework, several questions remain unanswered. The angle  $\theta_{23}$  produces nearly maximal mixing but has large uncertainties. If maximal, it would introduce an unexplained  $\mu$ – $\tau$  symmetry; should it differ from  $45^\circ$ , its octant would determine whether  $\nu_\tau$  or  $\nu_\mu$  couples more strongly to  $\nu_3$ . Furthermore, while it is known that the two independent mass splittings differ by a factor of 30, the sign of the larger splitting is unknown. The  $\nu_1$  and  $\nu_2$  states that contribute most to the  $\nu_e$  state could be lighter (“normal hierarchy”, NH) or heavier (“inverted hierarchy”, IH) than the  $\nu_3$  state. This question has important implications for models of neutrino mass [11–15] and for the study of the Dirac vs. Majorana nature of the neutrino [16, 17]. Additionally, neutrino mixing may be a source of CP violation if  $\sin \delta_{\text{CP}}$  is non-zero.

These questions can be addressed by the measurement of  $\nu_\mu \rightarrow \nu_\mu$ ,  $\bar{\nu}_\mu \rightarrow \bar{\nu}_\mu$ ,  $\nu_\mu \rightarrow \nu_e$ , and  $\bar{\nu}_\mu \rightarrow \bar{\nu}_e$  oscillations in matter over baselines  $L$  of order  $(100 - 1000) \text{ km}$ , with neutrino energies  $E[\text{GeV}] \simeq L[\text{km}] \cdot |\Delta m_{32}^2[\text{eV}^2/c^4]|$ . Several long-baseline experiments have reported observations of  $\nu_\mu \rightarrow \nu_\mu$  [18–21],  $\nu_\mu \rightarrow \nu_e$  [19–21], and  $\bar{\nu}_\mu \rightarrow \bar{\nu}_\mu$  [19, 20], but a statistically significant observation of  $\bar{\nu}_\mu \rightarrow \bar{\nu}_e$  has not previously been made. This report combines the first antineutrino measurements using the NOvA detectors with the neutrino data reported in Ref. [21] in a reoptimized analysis yielding a new determination of the oscillation parameters  $|\Delta m_{32}^2|$ ,  $\sin^2 \theta_{23}$ ,  $\delta_{\text{CP}}$ , and the neutrino mass hierarchy.

The NOvA experiment measures oscillations by comparing the energy spectra of neutrino interactions in two detectors placed in the Fermilab NuMI beam [22] at distances of 1 km (Near Detector, ND) and 810 km (Far Detector, FD) from the production target. The 14 kton FD measures  $15 \text{ m} \times 15 \text{ m} \times 60 \text{ m}$  while the 290 ton ND consists of a  $3.8 \text{ m} \times 3.8 \text{ m} \times 12.8 \text{ m}$  main detector followed by a muon range stack. Both detectors use liquid scintillator [23] contained in PVC cells that are  $6.6 \text{ cm} \times 3.9 \text{ cm}$  ( $0.15$  radiation lengths  $\times 0.45$  Molière radii) in cross section and span the height and width of the detectors in planes of alternating vertical and horizontal orientation. The ND is located 100 m underground. The FD oper-

ates on the surface with modest shielding resulting in 130 kHz of cosmic-ray activity. The detectors are located 14.6 mrad off the beam axis where the neutrino energy spectrum peaks at 2 GeV. Magnetic focusing horns in the beamline charge-select neutrino parents giving 96% (83%) pure  $\nu_\mu$  ( $\bar{\nu}_\mu$ ) event samples between 1 and 5 GeV. Most contamination is wrong-sign ( $\bar{\nu}$  in the  $\nu$  beam, or vice versa) with  $< 1\%$   $\nu_e + \bar{\nu}_e$  contamination.

This Letter reports data from an antineutrino beam run spanning from June 29, 2016 to February 26, 2019, with an exposure of  $12.33 \times 10^{20}$  protons-on-target (POT) delivered during 317.0 s of beam-on time, combined with the previously reported [21] neutrino beam exposure of  $8.85 \times 10^{20}$  POT and 438.2 s. During these periods, the proton source achieved a peak hourly-averaged power of 742 kW.

The flux of neutrinos delivered to the detectors is calculated using a simulation of the production and transport of particles through the beamline components [22, 24] and reweighted [25] to incorporate external measurements of hadron production and interactions [26–44]. Neutrino interactions in the detector are simulated using the GENIE event generator [45]. The cross section model has been tuned to improve agreement with external measurements and ND data, reducing uncertainties in the extrapolation of measurements in the ND to the FD. As in Ref. [21], we set  $M_A$  in the quasielastic dipole form factor to  $1.04 \text{ GeV}/c^2$  [46] and use corrections to the charged-current (CC) quasielastic cross section derived from the random phase approximation [47, 48]. In this analysis, we also apply this effect to baryon resonance production as a placeholder for the unknown nuclear effect that produces a suppression observed at low four-momentum transfer in our and other measurements [49–52]. Additionally, we increase the rate of deep-inelastic scattering with hadronic mass  $W > 1.7 \text{ GeV}/c^2$  by 10% to match our observed rates of short track-length  $\nu_\mu$  CC events. We model multi-nucleon ejection interactions following Ref. [53] and adjust the rates in bins of energy transfer,  $q_0$ , and 3-momentum transfer,  $|\vec{q}|$ , for  $\nu_\mu$  and  $\bar{\nu}_\mu$  separately to maximize agreement in the ND. The calculation of the  $\nu_e$  and  $\bar{\nu}_e$  rates uses these same models.

The energy depositions of final-state particles are simulated with GEANT4 [24] and input to a custom simulation of the production of, and the detector response to, scintillation and Cherenkov light [54]. The absolute energy scale of the detectors is calibrated to within  $\pm 5\%$  using the minimum ionizing portion of cosmic-ray muon tracks that stop in the detectors.

Cells with activity above threshold (hits) are grouped based on their proximity in space and time to produce candidate neutrino events. Events are assigned a vertex, and clusters are formed from hits likely to be associated with particles produced there [55]. These clusters are categorized as electromagnetic or hadronic in origin using a convolutional neural network (CNN) [56]. Hits forming

tracks are identified as muons by combining information on the track length,  $dE/dx$ , vertex activity, and scattering into a single particle identification (PID) score [57]. The same reconstruction algorithms are applied to events from data and simulation in both detectors.

The  $\nu_\mu$  and  $\bar{\nu}_\mu$  candidates are required to have a vertex inside the fiducial volume and no evidence of particles exiting the detector. The  $\nu_e$  and  $\bar{\nu}_e$  candidates are divided into a “core” sample which satisfies these containment requirements, and a “peripheral” sample which loosens these requirements for the most signal-like event topologies. A second CNN [58] serves as the primary PID, classifying event topologies as  $\nu_e$  CC,  $\nu_\mu$  CC,  $\nu_\tau$  CC, neutral-current (NC), or cosmic ray. The network is trained on simulated neutrino events and cosmic-ray data, separately for neutrino and antineutrino beam conditions. It has an improved architecture and higher rate of cosmic ray rejection over the previous network [21]. Events identified as  $\nu_\mu$  CC are further required to contain at least one track classified as a muon.

Several requirements further reduce cosmic-ray backgrounds. For the  $\nu_\mu$  CC sample, a boosted decision tree (BDT) algorithm based on vertex position and muon-like track properties is used. Events in the core  $\nu_e$  sample not aligned with the beam direction and that are near the top of the detector are rejected. Events characterized as detached bremsstrahlung showers from cosmic tracks are also removed, as are events whose topology is consistent with photons entering from the detector north side where there is less shielding. Events in the  $\nu_e$  peripheral sample are tested against a BDT classifier using event position and direction information to separate them from cosmic-ray topologies.

The selection of  $\nu_\mu$  and  $\bar{\nu}_\mu$  CC events is 31.2% (33.9%) efficient relative to true interactions in the fiducial volume, resulting in 98.6% (98.8%) pure samples at the FD during neutrino (antineutrino) beam operation. Both  $\nu_\mu$  and  $\bar{\nu}_\mu$  are counted as signal for the disappearance measurements. Selections against exiting particle tracks are the largest source of inefficiency. The efficiency for selecting signal  $\nu_e$  CC ( $\bar{\nu}_e$  CC) events is 62% (67%). Purities for the signal  $\nu_e$  ( $\bar{\nu}_e$ ) samples fall in the range 57–78% (55–77%) depending on the impact of oscillations on the signal and wrong-sign background levels. These efficiencies and purities differ from those quoted in Ref. [21] due to a reoptimization of the selection algorithms [59]. The wrong-sign component of the selected  $\nu_\mu$  sample in the ND is calculated to be  $2.8 \pm 0.3\%$  and  $10.6 \pm 1.1\%$  for the neutrino and antineutrino beams. These fractions were found to be consistent with a data-driven estimate based on the rate of  $\nu_\mu$  CC and NC interactions with associated detector activity indicative of neutron capture.

The incident neutrino energy is reconstructed from the measured energies of the final-state lepton and recoil hadronic system. The lepton energy is estimated from track length for muon candidates and from calorimetric

energy for electron candidates. The hadronic energy is estimated from the sum of the calibrated hits not associated with the primary lepton. The neutrino energy resolution at the FD is 9.1% (8.1%) for  $\nu_\mu$  CC ( $\bar{\nu}_\mu$  CC) events and 10.7% (8.8%) for  $\nu_e$  CC ( $\bar{\nu}_e$  CC) events. The  $\nu_\mu$  and  $\bar{\nu}_\mu$  events with the lowest hadronic energy fraction give the best energy resolution and lowest backgrounds, yielding the most precise measurement of the oscillated spectral shape, so we analyzed the spectra separately in quartiles of this variable [21].

The energy spectra of the selected  $\nu_\mu$  CC and  $\nu_e$  CC interactions in the ND during neutrino and antineutrino beam operations are shown in Fig. 1. The selected ND  $\nu_e$  sample consists entirely of background sources for the  $\nu_e$  appearance measurement, predominantly the intrinsic beam  $\nu_e$  component, along with misidentified  $\nu_\mu$  CC and NC interactions. We analyze the  $\nu_e$  candidate energy spectra in two bins of  $\nu_e$  PID (“low” and “high”) to isolate a highly pure sample of  $\nu_\mu \rightarrow \nu_e$  and  $\bar{\nu}_\mu \rightarrow \bar{\nu}_e$  at the FD. In the ND, the high-PID sample is dominated by intrinsic beam  $\nu_e$ . A third bin containing the “peripheral” events is added for the FD.

The  $\nu_\mu$  and  $\nu_e$  signal spectra at the FD are predicted for the neutrino and antineutrino beams separately and are based on the observed spectra of  $\nu_\mu$  candidate events in the ND. The true neutrino energy spectrum at the ND is estimated using the measured event rates in bins of reconstructed energy and the energy distributions of simulated events found to populate those bins. This true spectrum is corrected for differences in flux and acceptance between the ND and FD, as well as differences in the  $\nu_\mu$  and  $\nu_e$  cross sections; oscillations are then applied to yield predictions for the true  $\nu_\mu$  and  $\nu_e$  spectra at the FD. These spectra are then transformed into reconstructed energy using the underlying energy distributions from simulated neutrino interactions in the FD.

The predicted background spectra at the FD are also primarily data-driven. Data collected out-of-time with the NuMI beam provide a measurement of the rate of cosmic-ray backgrounds in the  $\nu_\mu$  and  $\nu_e$  samples. Neutrino backgrounds calculated to populate the FD  $\nu_e$  spectra are corrected based on the reconstructed  $\nu_e$  candidates at the ND. The procedure from Ref. [21] is followed to determine corrections for each background component in the neutrino-mode beam, while for the antineutrino-mode beam a single scale factor is used. The remaining backgrounds, which include any misidentified neutrino events in the  $\nu_\mu$  samples and misidentified  $\nu_\tau$  interactions in the  $\nu_e$  samples, make up less than 2% of the FD candidates and are taken directly from simulation.

To evaluate the impact of systematic uncertainties we recompute the extrapolation from the ND to the FD varying the parameters used to model the neutrino fluxes, neutrino cross sections, and the detector response. The procedure accounts for changes in the composition of the  $\nu_e$  background, and for impact on the transformation to

and from true and reconstructed energies due to variations in the model parameters. We parameterize each systematic variation and compute its effect in each analysis bin. These parameters are included in the oscillation fit constrained within their estimated uncertainties by penalty terms in the likelihood function.

TABLE I. Systematic uncertainties on the total predicted numbers of signal and beam-related background events at the best fit point (see Table IV) in the  $\nu_e$  selected samples in the neutrino and antineutrino datasets.

Source	$\nu_e$ Signal (%)	$\nu_e$ Bkg. (%)	$\bar{\nu}_e$ Signal (%)	$\bar{\nu}_e$ Bkg. (%)
Cross-sections	+4.7/-5.8	+3.6/-3.4	+3.2/-4.2	+3.0/-2.9
Detector model	+3.7/-3.9	+1.3/-0.8	+0.6/-0.6	+3.7/-2.6
ND/FD diffs.	+3.4/-3.4	+2.6/-2.9	+4.3/-4.3	+2.8/-2.8
Calibration	+2.1/-3.2	+3.5/-3.9	+1.5/-1.7	+2.9/-0.5
Others	+1.6/-1.6	+1.5/-1.5	+1.4/-1.2	+1.0/-1.0
Total	+7.4/-8.5	+5.6/-6.2	+5.8/-6.4	+6.3/-4.9

TABLE II. Systematic and statistical uncertainties on the oscillation parameters  $\sin^2 \theta_{23}$ ,  $\Delta m_{32}^2$ , and  $\delta_{\text{CP}}$ , evaluated at the best fit point (see Table IV).

Source	$\sin^2 \theta_{23}$ ( $\times 10^{-3}$ )	$ \Delta m_{32}^2 $ ( $\times 10^{-5} \text{ eV}^2/c^4$ )	$\delta_{\text{CP}}$ ( $\pi$ )
Calibration	+5.4 / -9.2	+2.2 / -2.6	+0.03 / -0.03
Neutron model	+6.0 / -13.0	+0.5 / -1.3	+0.01 / -0.00
Cross-sections	+4.1 / -7.7	+1.0 / -1.1	+0.06 / -0.07
$E_\mu$ scale	+2.3 / -3.0	+1.0 / -1.1	+0.00 / -0.00
Detector model	+1.9 / -3.2	+0.4 / -0.5	+0.05 / -0.05
Normalizations	+1.3 / -2.7	+0.1 / -0.2	+0.02 / -0.03
ND/FD diffs.	+1.0 / -4.0	+0.2 / -0.2	+0.06 / -0.07
Beam flux	+0.4 / -0.8	+0.1 / -0.1	+0.00 / -0.00
Total syst.	+9.7 / -20	+2.6 / -3.2	+0.11 / -0.12

The oscillation parameters that best fit the FD data are determined through minimization of a Poisson negative log-likelihood,  $-2 \ln \mathcal{L}$ , considering three unconstrained parameters,  $\Delta m_{32}^2$ ,  $\sin^2 \theta_{23}$ , and  $\delta_{\text{CP}}$ , as well as 53 constrained parameters covering the other PMNS oscillation parameters and the sources of systematic uncertainty summarized in Tables I and II. The two-detector design and extrapolation procedure significantly reduce the effect of the  $\simeq 10\text{--}20\%$  a priori uncertainties on the beam flux and cross sections. The principal remaining uncertainties are neutrino cross sections, the energy scale calibration, the detector response to neutrons, and differences between the ND and FD that cannot be corrected by extrapolation.

The selection criteria and techniques used in the analysis were developed on simulated data prior to inspection of the FD data distributions. Figure 1 shows the energy spectra of the  $\nu_\mu$  CC,  $\bar{\nu}_\mu$  CC,  $\nu_e$  CC, and  $\bar{\nu}_e$  CC candidates recorded at the FD overlaid on their oscillated best-fit expectations. Table III summarizes the total event

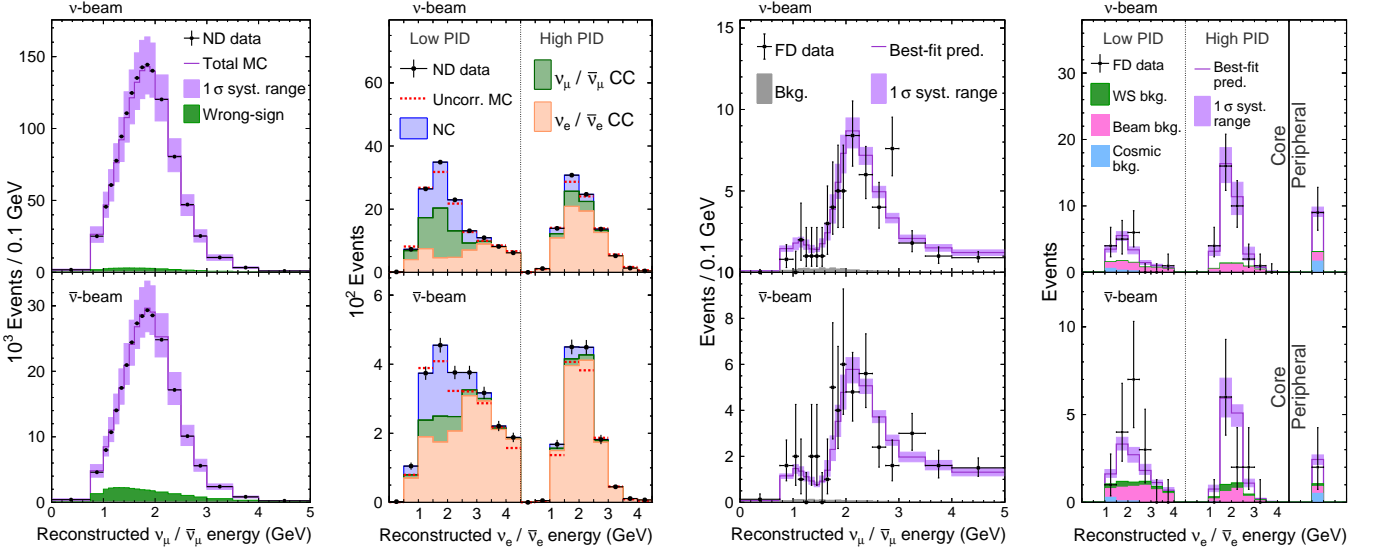


FIG. 1. From left to right, the reconstructed neutrino energy spectra for the ND  $\nu_\mu$  CC, ND  $\nu_e$  CC, FD  $\nu_\mu$  CC, FD  $\nu_e$  CC [60] with neutrino beam on the top and antineutrino beam on the bottom. For the ND  $\nu_\mu$  CC spectra, backgrounds aside from wrong-sign are negligible and not shown. The  $\nu_e$  CC spectra are split into a low and high purity sample, and the FD spectra shows counts in the “peripheral” sample. The dashed lines in the ND  $\nu_e$  spectra show the totals before data-driven corrections.

TABLE III. Event counts at the FD, both observed and predicted at the best fit point (see Table IV).

	Neutrino beam		Antineutrino beam	
	$\nu_\mu$ CC	$\nu_e$ CC	$\bar{\nu}_\mu$ CC	$\bar{\nu}_e$ CC
$\nu_\mu \rightarrow \nu_\mu$	112.5	0.7	24.0	0.1
$\bar{\nu}_\mu \rightarrow \bar{\nu}_\mu$	7.2	0.0	70.0	0.1
$\nu_\mu \rightarrow \nu_e$	0.1	44.3	0.0	2.2
$\bar{\nu}_\mu \rightarrow \bar{\nu}_e$	0.0	0.6	0.0	16.6
Beam $\nu_e + \bar{\nu}_e$	0.0	7.0	0.0	5.3
NC	1.3	3.1	0.8	1.2
Cosmic	2.1	3.3	0.8	1.1
Others	0.7	0.4	0.6	0.3
Signal	$120^{+10}_{-12}$	$44.3^{+3.5}_{-4.0}$	$93.9^{+8.1}_{-8.2}$	$16.6^{+0.9}_{-1.0}$
Background	$4.2^{+0.5}_{-0.6}$	$15.0^{+0.8}_{-0.9}$	$2.2^{+0.4}_{-0.4}$	$10.3^{+0.6}_{-0.5}$
Best fit	124	59.3	96.2	26.8
Observed	113	58	102	27

counts and estimated compositions of the selected samples. We recorded 102  $\bar{\nu}_\mu$  candidate events at the FD, reflecting a significant suppression from the unoscillated expectation of 476. We find 27  $\bar{\nu}_\mu \rightarrow \bar{\nu}_e$  candidate events with an estimated background of  $10.3^{+0.6}_{-0.5}$ , a  $4.4\sigma$  excess over the predicted background. This observation is the first evidence of  $\bar{\nu}_e$  appearance in a  $\bar{\nu}_\mu$  beam over a long baseline. These new antineutrino data are analyzed together with 113  $\nu_\mu$  and 58  $\nu_\mu \rightarrow \nu_e$  candidates from the previous data set.

Table IV shows the overall best-fit parameters, as well as the best fits for each choice of  $\theta_{23}$  octant and hierarchy. The best-fit point is found for the normal hierarchy with  $\theta_{23}$  in the upper octant where  $-2\ln\mathcal{L} = 157.1$  for

TABLE IV. Summary of oscillation parameters. The top three are inputs to this analysis [10], while the rest are the best fits for different choices of the mass hierarchy (NH, IH) and  $\theta_{23}$  octant (UO, LO), along with the significance (in units of  $\sigma$ ) at which those combinations are disfavored. In addition to the region indicated, for NH, LO a small range of  $\sin^2\theta_{23}$  0.45 – 0.48 is allowed at  $1\sigma$  [61].

$\Delta m_{21}^2 / (10^{-5} \text{ eV}^2/c^4)$	$7.53 \pm 0.18$			
$\sin^2\theta_{12}$	$0.307^{+0.013}_{-0.012}$			
$\sin^2\theta_{13}$	$0.0210 \pm 0.0011$			
$\Delta m_{32}^2 / (10^{-3} \text{ eV}^2/c^4)$	NH, UO	NH, LO	IH, UO	IH, LO
	$+2.48^{+0.11}_{-0.06}$	$+2.47$	$-2.54$	$-2.53$
	$\sin^2\theta_{23}$	$0.56^{+0.04}_{-0.03}$	0.48	0.56
	$\delta_{\text{CP}}/\pi$	$0.0^{+1.3}_{-0.4}$	1.9	1.5
	-	$+1.6\sigma$	$+1.8\sigma$	$+2.0\sigma$

175 degrees of freedom (goodness-of-fit  $p = 0.91$  from simulated experiments). The measured values of  $\theta_{23}$  and  $\Delta m_{32}^2$  are consistent with the previous NOvA measurement [21] that used only neutrino data, and are consistent with maximal mixing within  $1.2\sigma$ .

Confidence intervals for the oscillation parameters are determined using the unified approach [65], as detailed in Ref. [66]. Figure 2 compares the 90% confidence level contours in  $\Delta m_{32}^2$  and  $\sin^2\theta_{23}$  with those of other other experiments [19, 20, 62, 63]. Figure 3 shows the allowed regions in  $\sin^2\theta_{23}$  and  $\delta_{\text{CP}}$ . These results exclude most values near  $\delta_{\text{CP}} = \pi/2$  in the inverted mass hierarchy by more than  $3\sigma$ ; specifically the intervals between  $-0.04$  to  $0.97\pi$  in the lower  $\theta_{23}$  octant and  $0.04$  to  $0.91\pi$  in the upper octant. The data prefer the normal hierarchy

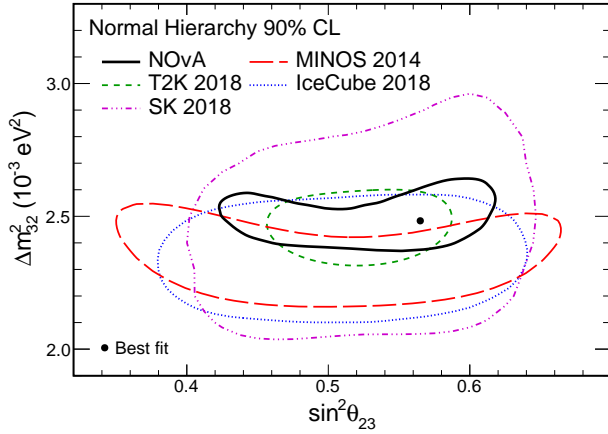


FIG. 2. The 90% confidence level region for  $\Delta m_{32}^2$  and  $\sin^2 \theta_{23}$ , with best-fit point shown as a black marker [61], overlaid on contours from other experiments [19, 20, 62, 63].

with a significance of  $1.9\sigma$  ( $p = 0.057$ ,  $CL_s = 0.091$  [67]) and the upper  $\theta_{23}$  octant with a significance of  $1.6\sigma$  ( $p = 0.11$ ), profiling over all other parameter choices.

We are grateful to Stephen Parke (FNAL) for useful discussions. This document was prepared by the NOvA collaboration using the resources of the Fermi National Accelerator Laboratory (Fermilab), a U.S. Department of Energy, Office of Science, HEP User Facility. Fermilab is managed by Fermi Research Alliance, LLC (FRA), acting under Contract No. DE-AC02-07CH11359. This work was supported by the U.S. Department of Energy; the U.S. National Science Foundation; the Department of Science and Technology, India; the European Research Council; the MSMT CR, GA UK, Czech Republic; the RAS, RFBR, RMES, RSF, and BASIS Foundation, Russia; CNPq and FAPEG, Brazil; STFC, and the Royal Society, United Kingdom; and the state and University of Minnesota. This work used resources of the National Energy Research Scientific Computing Center (NERSC), a U.S. Department of Energy Office of Science User Facility operated under Contract No. DE-AC02-05CH11231. We are grateful for the contributions of the staffs of the University of Minnesota at the Ash River Laboratory and of Fermilab.

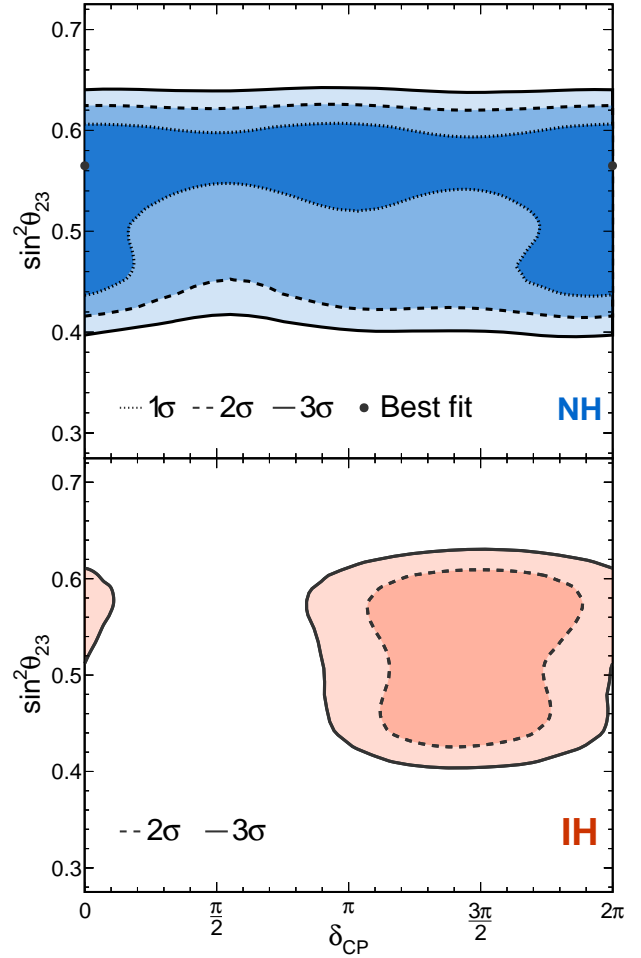


FIG. 3. The  $1\sigma$ ,  $2\sigma$ , and  $3\sigma$  contours in  $\sin^2 \theta_{23}$  vs.  $\delta_{CP}$  in the normal hierarchy (NH, top panel) and inverted hierarchy (IH, bottom panel) [64]. The best-fit point is shown by a black marker.

[1] Y. Fukuda *et al.* (Super-Kamiokande), Phys. Rev. Lett. **81**, 1562 (1998), arXiv:hep-ex/9807003 [hep-ex].  
[2] S. Fukuda *et al.* (Super-Kamiokande), Phys. Lett. **B539**, 179 (2002), arXiv:hep-ex/0205075 [hep-ex].  
[3] Q. R. Ahmad *et al.* (SNO), Phys. Rev. Lett. **89**, 011301 (2002), arXiv:nucl-ex/0204008 [nucl-ex].  
[4] K. Eguchi *et al.* (KamLAND), Phys. Rev. Lett. **90**, 021802 (2003), arXiv:hep-ex/0212021 [hep-ex].  
[5] D. G. Michael *et al.* (MINOS), Phys. Rev. Lett. **97**,

191801 (2006), arXiv:hep-ex/0607088 [hep-ex].  
[6] K. Abe *et al.* (T2K), Phys. Rev. Lett. **107**, 041801 (2011), arXiv:1106.2822 [hep-ex].  
[7] Y. Abe *et al.* (Double Chooz), Phys. Rev. Lett. **108**, 131801 (2012), arXiv:1112.6353 [hep-ex].  
[8] F. P. An *et al.* (Daya Bay), Phys. Rev. Lett. **108**, 171803 (2012), arXiv:1203.1669 [hep-ex].  
[9] J. K. Ahn *et al.* (RENO), Phys. Rev. Lett. **108**, 191802 (2012), arXiv:1204.0626 [hep-ex].  
[10] C. Patrignani *et al.* (Particle Data Group), Chin. Phys. **C40**, 100001 (2016), and 2017 update.  
[11] R. N. Mohapatra and A. Y. Smirnov, *Elementary particle physics. Proceedings, Corfu Summer Institute, CORFU2005, Corfu, Greece, September 4-26, 2005*, Ann. Rev. Nucl. Part. Sci. **56**, 569 (2006), arXiv:hep-ph/0603118 [hep-ph].  
[12] H. Nunokawa, S. J. Parke, and J. W. F. Valle, Prog. Part. Nucl. Phys. **60**, 338 (2008), arXiv:0710.0554 [hep-ph].  
[13] G. Altarelli and F. Feruglio, Rev. Mod. Phys. **82**, 2701

- (2010), arXiv:1002.0211 [hep-ph].
- [14] S. F. King, J. Phys. **G42**, 123001 (2015), arXiv:1510.02091 [hep-ph].
- [15] S. T. Petcov, Eur. Phys. J. **C78**, 709 (2018), arXiv:1711.10806 [hep-ph].
- [16] S. Pascoli and S. T. Petcov, Phys. Lett. **B544**, 239 (2002), arXiv:hep-ph/0205022 [hep-ph].
- [17] J. N. Bahcall, H. Murayama, and C. Pena-Garay, Phys. Rev. **D70**, 033012 (2004), arXiv:hep-ph/0403167 [hep-ph].
- [18] M. H. Ahn *et al.* (K2K), Phys. Rev. **D74**, 072003 (2006), arXiv:hep-ex/0606032 [hep-ex].
- [19] P. Adamson *et al.* (MINOS), Phys. Rev. Lett. **112**, 191801 (2014), arXiv:1403.0867 [hep-ex].
- [20] K. Abe *et al.* (T2K), Phys. Rev. Lett. **121**, 171802 (2018), arXiv:1807.07891 [hep-ex].
- [21] M. A. Acero *et al.* (NOvA), Phys. Rev. **D98**, 032012 (2018), arXiv:1806.00096 [hep-ex].
- [22] P. Adamson *et al.*, Nucl. Instrum. Meth. **A806**, 279 (2016), arXiv:1507.06690 [physics.acc-ph].
- [23] S. Mufson *et al.*, Nucl. Instrum. Meth. **A799**, 1 (2015), arXiv:1504.04035 [physics.ins-det].
- [24] S. Agostinelli *et al.* (GEANT4), Nucl. Instrum. Meth. **A506**, 250 (2003).
- [25] L. Aliaga *et al.* (MINERvA), Phys. Rev. **D94**, 092005 (2016), [Addendum: Phys. Rev. **D95**, no.3, 039903 (2017)], arXiv:1607.00704 [hep-ex].
- [26] J. M. Paley *et al.* (MIPP), Phys. Rev. **D90**, 032001 (2014), arXiv:1404.5882 [hep-ex].
- [27] C. Alt *et al.* (NA49), Eur. Phys. J. **C49**, 897 (2007), arXiv:hep-ex/0606028 [hep-ex].
- [28] N. Abgrall *et al.* (NA61/SHINE), Phys. Rev. **C84**, 034604 (2011), arXiv:1102.0983 [hep-ex].
- [29] D. S. Barton *et al.*, Phys. Rev. **D27**, 2580 (1983).
- [30] S. M. Seun, *Measurement of  $\pi - K$  ratios from the NuMI target*, Ph.D. thesis, Harvard U. (2007).
- [31] G. M. Tinti, *Sterile neutrino oscillations in MINOS and hadron production in pC collisions*, Ph.D. thesis, Oxford U. (2010).
- [32] A. V. Lebedev, *Ratio of pion kaon production in proton carbon interactions*, Ph.D. thesis, Harvard U. (2007).
- [33] B. Baatar *et al.* (NA49), Eur. Phys. J. **C73**, 2364 (2013), arXiv:1207.6520 [hep-ex].
- [34] P. Skubic *et al.*, Phys. Rev. **D18**, 3115 (1978).
- [35] S. P. Denisov, S. V. Donskov, Yu. P. Gorin, R. N. Krasnokutsky, A. I. Petrukhin, Yu. D. Prokoshkin, and D. A. Stoyanova, Nucl. Phys. **B61**, 62 (1973).
- [36] A. S. Carroll *et al.*, Phys. Lett. **80B**, 319 (1979).
- [37] K. Abe *et al.* (T2K), Phys. Rev. **D87**, 012001 (2013), [Addendum: Phys. Rev. **D87**, no.1, 019902 (2013)], arXiv:1211.0469 [hep-ex].
- [38] T. K. Gaisser, G. B. Yodh, V. D. Barger, and F. Halzen, in *14th International Cosmic Ray Conference (ICRC 1975) Munich, Germany, August 15-29, 1975* (1975) pp. 2161–2166.
- [39] J. W. Cronin, R. Cool, and A. Abashian, Phys. Rev. **107**, 1121 (1957).
- [40] J. V. Allaby *et al.* (IHEP-CERN), Phys. Lett. **30B**, 500 (1969).
- [41] M. J. Longo and B. J. Moyer, Phys. Rev. **125**, 701 (1962).
- [42] B. M. Bobchenko *et al.*, Sov. J. Nucl. Phys. **30**, 805 (1979), [Yad. Fiz. **30**, 1553 (1979)].
- [43] V. B. Fedorov, Yu. G. Grishuk, M. V. Kosov, G. A. Leksin, N. A. Pivnyuk, S. V. Shevchenko, V. L. Stolin, A. V. Vlasov, and L. S. Vorobev, Sov. J. Nucl. Phys. **27**, 222 (1978), [Yad. Fiz. **27**, 413 (1978)].
- [44] R. J. Abrams, R. L. Cool, G. Giacomelli, T. F. Kycia, B. A. Leontic, K. K. Li, and D. N. Michael, Phys. Rev. **D1**, 1917 (1970).
- [45] C. Andreopoulos *et al.*, Nucl. Instrum. Meth. **A614**, 87 (2010), this work uses version 2.12.2, arXiv:0905.2517 [hep-ph].
- [46] A. S. Meyer, M. Betancourt, R. Gran, and R. J. Hill, Phys. Rev. **D93**, 113015 (2016), arXiv:1603.03048 [hep-ph].
- [47] J. Nieves, J. E. Amaro, and M. Valverde, Phys. Rev. **C70**, 055503 (2004), [Erratum: Phys. Rev. **C72**, 019902 (2005)], arXiv:nucl-th/0408005 [nucl-th].
- [48] R. Gran, (2017), arXiv:1705.02932 [hep-ex].
- [49] P. Adamson *et al.* (MINOS), Phys. Rev. **D91**, 012005 (2015), arXiv:1410.8613 [hep-ex].
- [50] A. A. Aguilar-Arevalo *et al.* (MiniBooNE), Phys. Rev. **D83**, 052007 (2011), arXiv:1011.3572 [hep-ex].
- [51] C. L. McGivern *et al.* (MINERvA), Phys. Rev. **D94**, 052005 (2016), arXiv:1606.07127 [hep-ex].
- [52] O. Altinok *et al.* (MINERvA), Phys. Rev. **D96**, 072003 (2017), arXiv:1708.03723 [hep-ex].
- [53] T. Katori, *Proceedings, 8th International Workshop on Neutrino-Nucleus Interactions in the Few GeV Region (NuInt 12): Rio de Janeiro, Brazil, October 22-27, 2012*, AIP Conf. Proc. **1663**, 030001 (2015), arXiv:1304.6014 [nucl-th].
- [54] A. Aurisano, C. Backhouse, R. Hatcher, N. Mayer, J. Musser, R. Patterson, R. Schroeter, and A. Sousa (NOvA), *Proceedings, 21st International Conference on Computing in High Energy and Nuclear Physics (CHEP 2015): Okinawa, Japan, April 13-17, 2015*, J. Phys. Conf. Ser. **664**, 072002 (2015).
- [55] M. Baird, J. Bian, M. Messier, E. Niner, D. Rocco, and K. Sachdev, *Proceedings, 21st International Conference on Computing in High Energy and Nuclear Physics (CHEP 2015): Okinawa, Japan, April 13-17, 2015*, J. Phys. Conf. Ser. **664**, 072035 (2015).
- [56] F. Psihas, *Measurement of Long Baseline Neutrino Oscillations and Improvements from Deep Learning*, Ph.D. thesis, Indiana U. (2018).
- [57] N. J. Raddatz, *Measurement of Muon Neutrino Disappearance with Non-Fiducial Interactions in the NOvA Experiment*, Ph.D. thesis, Minnesota U. (2016).
- [58] A. Aurisano, A. Radovic, D. Rocco, A. Himmel, M. D. Messier, E. Niner, G. Pawloski, F. Psihas, A. Sousa, and P. Vahle, JINST **11**, P09001 (2016), arXiv:1604.01444 [hep-ex].
- [59] T. Blackburn, *Measurement of  $\Delta m_{32}^2$  and  $\sin^2 \theta_{23}$  using Muon Neutrino and Antineutrino Beams in the NOvA Experiment*, Ph.D. thesis, Sussex U. (2019).
- [60] See Supplemental Material at [URL will be inserted by publisher] for the muon neutrino distributions in each quartile of hadronic energy fraction (2019).
- [61] See Supplemental Material at [URL will be inserted by publisher] for the profiles of these surfaces on the  $\Delta m_{32}^2$  and  $\sin^2 \theta_{23}$  axes as well as the surfaces computed for the inverted hierarchy case (2019).
- [62] K. Abe *et al.* (Super-Kamiokande), Phys. Rev. **D97**, 072001 (2018), arXiv:1710.09126 [hep-ex].
- [63] M. G. Aartsen *et al.* (IceCube), Phys. Rev. Lett. **120**, 071801 (2018), arXiv:1707.07081 [hep-ex].
- [64] See Supplemental Material at [URL will be inserted by

- publisher] for profiles of these surfaces on the  $\delta_{\text{CP}}$  axis (2019).
- [65] G. J. Feldman and R. D. Cousins, Phys. Rev. **D57**, 3873 (1998), arXiv:physics/9711021 [physics.data-an].
- [66] A. Sousa, N. Buchanan, S. Calvez, P. Ding, D. Doyle, H. Alexander, B. Holzman, J. Kowalkowski, A. Norman, and T. Peterka, in *Proceedings of the 23rd International Conference on Computing in High-Energy and Nuclear Physics (CHEP 2018)*, Sofia, Bulgaria, July 9-13, 2018 (2019) in press.
- [67] A. L. Read, *Advanced Statistical Techniques in Particle Physics. Proceedings, Conference, Durham, UK, March 18-22, 2002*, J. Phys. **G28**, 2693 (2002), [,11(2002)].